Fecal virome transfer improves proliferation of commensal gut *Akkermansia muciniphila* and unexpectedly enhances the fertility rate in laboratory mice

Torben Sølbeck Rasmussen[1*], Caroline M. Junker Mentzel[2], Malene Refslund Danielsen[1], Rasmus Riemer Jakobsen[1], Line Sidsel Fisker Zachariassen[2], Josue Leonardo Castro Mejia[1], Lars Hestbjerg Hansen[3], Axel Kornerup Hansen[2], Dennis Sandris Nielsen[1*]

1 Section of Microbiology and Fermentation, Dept. of Food Science, University of Copenhagen, Frederiksberg, Denmark

2 Section of Experimental Animal Models, Dept. of Veterinary and Animal Sciences, University of Copenhagen, Frederiksberg, Denmark

3 Section of Microbial Ecology and Biotechnology, Department of Plant and Environmental Sciences, University of Copenhagen, Frederiksberg, Denmark

**Address correspondence to dn@food.ku.dk (+45 35 33 32 87) / torben@food.ku.dk (+45 35 32 80 73), Rolighedsvej 26 4th floor, 1958 Frederiksberg C, Denmark.*

Keywords: Fecal virome transplantation, gut microbiota, fertility, probiotic engraftment, *Lacticaseibacillus rhamnosus, Akkermansia muciniphila*

Abstract

Probiotics have been suggested as nutritional supplements to improve gastrointestinal health. However, the probiotics marketed today only colonize the densely populated gut to a limited extent. Bacteriophages comprise the majority of viruses in the human gut virome and there are strong indications that they play important roles in shaping the gut microbiome (GM). Here we investigate the use of fecal virome transplantation (FVT) as a mean to alter GM composition to lead the way for persistent colonization of two types of probiotics: *Lacticaseibacillus rhamnosus* GG (LGG) representing a well-established probiotic and *Akkermansia muciniphila* (AKM) representing a putative next-generation probiotic. Male and female C57BL/6NTac mice were cohoused in pairs at 4 weeks of age and received the following treatment by oral gavage at week 5 and 6: AKM+FVT, probiotic sham (Pro-sham)+FVT, LGG+Saline, AKM+Saline, and control (Pro-sham+Saline). The FVT originated from donor mice with high relative abundance of *A. muciniphila*. All animals were terminated at age 9 weeks. The FVT treatment did not increase the relative abundance of the administered LGG or AKM in the recipient mice. Instead FVT significantly ($p<0.05$) increased the abundance of naturally occurring *A. muciniphila* compared to the control. This highlights the potential of stimulating the commensal "probiotics" that already are permanent members of the gut. Being co-housed male and female, a fraction of the female mice became pregnant. Unexpectedly, the FVT treated mice were found to have a significantly ($p<0.05$) higher fertility rate independent of probiotic administration. These preliminary observations urge for follow-up studies investigating GM/fertility interactions.

Introduction

During the last decade it has become commonly accepted that gut microbiome (GM) imbalances (dysbiosis) play important roles in the etiology of a number of diseases [1–3]. Probiotics has been suggested as a tool to restore GM balance [4,5] and are defined as live microorganisms that when ingested in adequate amounts confer a health benefit to the host [6]. However, traditional probiotics, mainly lactobacilli and bifidobacteria, in general have no or only modest influence on GM composition [7]. So-called next generation probiotics, like *Akkermansia muciniphila*, have recently been suggested for alleviating GM-associated malfunctions [8,9]. Persistent beneficial effects are challenged by the difficulties of the administered bacteria to become a permanent and adequately abundant member of the densely populated GM [10,11].

Mounting evidence suggests that the gut viral community plays a pivotal role in shaping the composition of the GM [12,13]. The gut virome is predominated by prokaryotic viruses [14], including bacteriophages (phages), which are viruses that attack bacteria in a host-specific manner [15]. A transfer of sterile filtered feces (containing phages, but no intact bacterial cells) from a healthy donor have shown to successfully treat recurrent *Clostridioides difficile* infections (rCDI) in human recipients [16]. Other studies using sterile filtered feces have reported to alleviate symptoms of type-2-diabetes (T2D) and obesity in mice [17], and to prevent the development of necrotizing enterocolitis [18] in preterm piglets. These changes in phenotype may be driven by a phage-mediated modulation of the GM [17–21]. In all cases, when transferring the fecal viral components, a significant change in the bacterial diversity and composition was observed, with the bacterial GM-component of the recipients becoming more like the GM of the donors. We will refer to this approach as fecal virome transplantation (FVT).

Using co-housed male and female laboratory mice as model, we hypothesized that initial phage-mediated disturbance of the existing bacterial landscape in the GM (using FVT) would improve the enteric engraftment and abundance of the administered probiotic bacteria (*Lactocaseibacillus rhamnosus* GG or *A. muciniphila*). We did the following considerations to maximize our chances for evaluating a successful enteric engraftment of *A. muciniphila*: (i) C57BL/6NTac (B6N mice from Taconic) mice were selected since previous experience have shown a low relative abundance of *A. muciniphila* in mice from this vendor [22], (ii) the *A. muciniphila* YL-44 strain was used in this study due to its enteric origin from the genetically close related C57BL/6J (B6J) wildtype mouse, and (iii) the FVT virome represented a gut virome from mice donors with relatively high *A. muciniphila* abundance [22].

Results

Here we investigated the potential of transferring an *A. muciniphila* rich GM phenotype via fecal virome transplantation (FVT) from lean mouse donors to lean recipients to improve persistent colonization of two probiotics; *L. rhamnosus GG* (LGG) or *A. muciniphila* (AKM). Fecal samples from three different timepoints were included to investigate the level of probiotic engraftment and GM changes over time: baseline, 6 days after 2nd intervention, and at termination. See Figure 1 for the experimental design of the animal model.

FVT enhanced the abundance of natural occurring Akkermansia muciniphila strains

Our hypothesis was that initial disruption of the GM landscape driven by the FVT would lead to an increase in the abundance of AKM and/or LGG after probiotic administration. However, we did not observe any significant effect of the FVT on the AKM/LGG abundance after intervention nor at termination (Figure 2). Instead, we observed at termination that FVT had increased ($p < 0.05$) the abundance of, what would be expected to be, naturally occurring (native) *A. muciniphila* strains in mice that were not provided AKM as probiotic compared to mice neither provided FVT nor AKM (Figure 2A & Figure 2C). The abundance of *A. muciniphila* strains at baseline were significantly lower ($p < 0.05$) compared to termination in AKM+FVT and Pro-sham+FVT mice, while tending lower ($p < 0.1$) in the LGG+FVT mice as well (Figure S1).

This indicated that the FVT had improved the growth conditions of naturally occurring *A. muciniphila* strains due to yet unknown environmental changes. The AKM+Saline mice had similar *A. muciniphila* abundance as the FVT groups. Additional experiments were performed to rule out that the FVT initially contained any *A. muciniphila* strains (Figure S2). The sterile filtered donor feces (used for FVT) were incubated in 96 hours on GAM agar plates from which eight colonies appeared. Cell morphology of these colonies was imaged with phase-contrast microscopy, and subsequently screened with *A. muciniphila* specific primers in both a PCR and qPCR assay. Neither colony morphology, cell morphology, PCR nor qPCR indicated any traces of *A. muciniphila* in the applied donor FVT (Figure S2).

FVT leads to a reduction in bacterial diversity of the GM component

FVT significantly ($p < 0.05$) decreased the bacterial Shannon diversity index in the LGG+FVT and Pro-sham+FVT mice at termination (9 weeks of age) when compared with the AKM+Saline, LGG+Saline, and the control mice (Figure 3A). Whereas the Shannon diversity index of the

AKM+FVT mice remained unchanged compared to the control mice, hence suggesting that AKM may have counteracted the decrease in the Shannon diversity that was associated to the FVT treatment (Figure 3A). The initial bacterial diversity at baseline was similar between all groups (Figure 2A). The most abundant genus in all groups at all time-points were *Lactobacillus* (Figure S3). The FVT-associated differences in the bacterial Shannon diversity index were not reflected in the bacterial composition analysis (Bray-Curtis dissimilarity), since no significant differences were observed between treatments at all three timepoints (Figure 3B). Probably due to the state of pregnancy, the sex of the animals (male vs female) showed significant ($p < 0.001$) differences in their bacterial composition at termination (Figure S4). Differential abundance (DA) analysis showed that *Candidatus* Arhtromitus (segmented filamentous bacteria) and *A. muciniphila* amplicon sequence variants (ASVs) were significantly ($p < 0.05$) increased in relative abundance at termination in mice receiving FVT compared to the other groups (Figure 3C). Thus, clearly supporting the FVT-mediated enhancement of *A. muciniphila* abundance measured by the qPCR analysis. The administration of AKM significantly increased ($p < 0.05$) the relative abundance of *Ruminococcus gnavus* (Figure S5) but not *per se* influence *A. muciniphila* relative abundance in the recipients.

Probiotic and FVT intervention may have changed the viral GM profile

The viral Shannon diversity index at termination (9 weeks of age) was affected by FVT ($p = 0.032$) as well as the administration of the probiotics AKM (tendency, $p = 0.07$) and LGG ($p = 0.006$) when compared to the control mice (Figure 4A and Figure S6). The effects of AKM ($p = 0.025$) and LGG ($p = 0.014$) were also reflected on the viral composition at termination (Figure S7). The sex of the animals appeared to influence ($p < 0.05$) the viral community composition across all time points (Figure S4). The donor FVT virome consisted of more than 90% *Microviridae* viruses and was markedly different in both viral diversity and composition (Figure 4A & Figure 4B) compared to the recipient gut virome (Figure S8). DA analysis was performed using both the predicted bacterial hosts and raw viral taxonomy at termination (9 weeks of age). These analyzes showed a significant increase in the relative abundance of predicted hosts belonging of the taxa *Lachnospiraceae*, *Parabacteroides*, and *Bacteroides* in FVT treated mice (Figure S9), and an increase in the relative abundance of *Petitvirales* (likely *Microviridae*) when comparing with mice not receiving FVT (Figure 4C). It could be speculated that the elevated level of *Petitvirales* in the FVT treated mice was driven by the highly *Microviridae* abundant (> 90% of relative abundance) donor virome.

The viral Shannon diversity at baseline of the AKM+FVT and Pro-sham+FVT mice were significantly lower ($p < 0.05$) compared to control (Figure 4A), while the diversity of the remaining treatment groups was similar to the control mice. This initial variance also tended to be reflected ($p < 0.084$) on the viral composition at baseline, but these differences were diminished at termination (Figure 4B). The extent to which the above-mentioned inter-group differences were associated with the baseline variance of viral diversity and composition was not clear.

A. muciniphila affects expression of a gene involved in mucin-production and limits an inflammatory response associated to FVT

The ileum tissue was investigated for changes in the expression levels of genes associated to inflammatory responses. Interestingly, mice with the highest abundance at termination of the mucin-degrading *A. muciniphila* (Figure 2A) had either significantly ($p < 0.05$, AKM+Saline and AKM+FVT) or tended towards ($p < 0.1$, LGG+FVT) lowered gene expression of genes related to inflammatory responses compared to control mice (Figure 5A). The *Muc1* gene is involved in mucin production [23]. Whether this affected the mouse phenotype was not clear. The expression of nine genes that are involved in inflammation and as a response on infection (*Clc2*, *Ccr10*, *Ctla4*, *Cxcl1*, *Il1b*, *Il4*, Il6*, Retnlb*, *Timp1)*, were significantly ($p < 0.05$) elevated in Pro-sham+FVT compared to control mice (Figure 5A - 5J). Additionally, two genes (*Ffar2* and *Ffar3*) involved in both energy homeostasis and intestinal immunity were respectively increased (tendency, $p = 0.06$) or decreased ($p = 0.01$) in the Pro-sham+FVT compared to control mice (Figure 5K & 5L). Excluding the Pro-sham+FVT mice, the *nod2* gene was lowered in expression in all treatment groups compared to control (Figure 5M).

Altogether, these changes in gene expression indicate that the FVT of the Pro-sham+FVT mice had initiated an inflammatory response, possibly mediated by the presence of eukaryotic and/or prokaryotic viruses that were transferred with the FVT. The administration of AKM along with FVT seemed to counteract this inflammatory response, since the expression of none of the above-mentioned 11 genes were changed in the AKM+Saline or AKM+FVT compared to control mice (Figure 5A – 5L).

Fluorescence-activated cell sorting (FACS) was performed to evaluate the presence of selected immune cells in the mesenteric lymph node (MLN) at termination. The FVT treated male and female mice expressed a significant ($p = 0.043$) decrease in the total number of T cells ($CD3^+$ lymphocytes) (Figure 5N), while mice provided only LGG had a significant decrease ($p = 0.01$) in the level of

cytotoxic T cells ($CD8^+/CD3^+$) (Figure 5O). The level of cytotoxic T cells in the MLN was not affected by the FVT treatment, suggesting that the increased expression of inflammatory genes in the ileum tissue, isolated from the Pro-sham+FVT mice, was not a systemic response. The levels of the remaining measured immune cells (CD11c, $CD86^+CD11c$, $CD11b^+CD11c$, $CD103^+CD11c$) were not significantly affected by the sex of the animals, probiotics (AKM/LGG) or FVT.

Increased fertility rate following FVT

The pregnancy status and fertility rate (number of fetuses or born pups) were evaluated for each female mouse (Figure 6 and Figure S10) due to the natural consequences of pairing male and female mice in cages. Surprisingly, the FVT treated female mice (Pro-sham+FVT, AKM+FVT, and LGG+FVT) exhibited a significant increase in both fertility rate ($p = 0.014$, Figure 6A) and pregnancy status ($p = 0.025$), Figure 6B) compared to controls. These observations were independent of the administered probiotics LGG/AKM. It was also observed that none of the female AKM+Saline mice ($n = 4$) were pregnant (Figure S10).

Discussion

Here we investigated the potential of using phage-mediated "GM disturbance" to improve the engraftment of two different probiotics (*A. muciniphila;* AKM and *L. rhamnosus GG;* LGG) in lean mouse recipients over a time span of 5 weeks. The hypothesis was that fecal virome transplantation (FVT) followed by probiotic administration would increase the chance of persistent enteric colonization of the probiotic bacteria. However, the results did not support the hypothesis. Instead, specie specific qPCR analysis showed that the FVT treatment at termination (9 weeks of age) had significantly ($p < 0.05$) increased the abundance of naturally occurring *A. muciniphila* strains, compared to non-FVT treated mice (Figure 2A & 2C). We ruled out that other *A. muciniphila* strains were present in the applied FVT virome (Figure S2). The control (Pro-sham+Saline) and LGG+Saline mice also increased their *A. muciniphila* abundance over time which likely can be explained by regular GM maturation [24,25]. However, *A. muciniphila* abundance remained 1-2 log higher ($p = 0.065$) in the FVT/AKM groups at termination compared with the mice receiving neither AKM nor FVT (Figure S1). The applied FVT originated from a GM community that allowed a relative abundance of *A. muciniphila* > 6% [22]. Hence, the FVT-mediated enhancement of the abundance of naturally occurring *A. muciniphila* strains emphasize the potential of transferring a phenotype along

with the FVT. A concept which has been reported in other studies as well [16–19]. The administered LGG did not persistently colonize regardless of FVT treatment (Figure 2).

The bacteriome analysis showed that FVT significantly ($p < 0.05$) decreased the bacterial Shannon diversity in the LGG+FVT and Pro-sham+FVT mice at termination compared to the control and the other treatment groups (Figure 3A). However, AKM may have counteracted this tendency since the bacterial diversity of the AKM+FVT was unaffected. The mechanism behind this observation is unknown. However, assuming that a phenotype can be transferred along with the FVT, the decrease in bacterial diversity may be associated to the very low viral diversity and markedly different viral composition in the transferred FVT donor virome (Figure 4A & 4B). It could therefore be hypothesized that a low viral diversity may also favor a low bacterial diversity, due to the inherit link between phages and their bacterial hosts. This may fit with a previous study where the viral diversity of the fecal donor virome was higher than the recipient virome and FVT resulted in increased bacterial diversity in the recipient mice compared to non-FVT treated mice [17]. More than 90% of the relative abundance of the FVT donor virome represented *Microviridae* viruses which was in accordance to the relative abundance of genetically identical B6N mice in a previous study [22]. Furthermore, PhiX (a *Microviridae* used to spike the metavirome sequencing) sequences were excluded from the analysis, thus the high relative abundance of *Microviridae* was not a technical artefact.

It should be noted that the initial viral diversity and composition at baseline appeared to vary within the treatment groups. The interpretation of changes in the viral diversity and composition were therefore challenged, although the analysis indicated that the FVT, AKM, and/or LGG may have affected ($p < 0.05$) both the viral Shannon diversity and composition irrespectively of initial group differences.

Both immune cell counting and the expression levels of genes involved inflammatory responses were measured to evaluate potential safety issues associated to the FVT from lean donors to lean recipients. Here especially the Pro-sham+FVT appeared with significantly ($p < 0.05$) increased gene expression levels compared to control mice (Figure 5) in the following pro- and/or anti-inflammatory related genes; *Ccl2* [26], *Ccr10* [27], *Ctla4* [28], *Cxcl1* [29], *Il1b* [30], *Il4* [31], *Il6* [32], *Retnlb* [33], *Timp1* [34], *Ffar2* [35,36], whereas *Ffar3* [35] and *Nod2* [37] decreased. Interestingly, the combination of AKM+FVT counteracted the elevated expression of these genes (Figure 5), which may be explained by previously suggested synergistic effects of combining probiotics and phages [38]. These indications of inflammatory response in the ileum tissue were not supported by immune

cell counts in the mesenteric lymph node (MLN). The T cell counts were significantly lower ($p < 0.05$) in FVT treated mice compared to the control while the cytotoxic T cell and dendritic cell counts were similar when compared to control mice (Figure 5N & 5O). This suggest that the FVT did not activate a systemic immune response, but rather a more a local response due to the presence of foreign viral particles [39,40].

The administration of AKM in the AKM+Saline and AKM+FVT mice significantly decreased ($p < 0.05$) the expression of the *Muc1* gene that is a membrane-tethered mucin expressed on surfaces of epithelial cells – also in the intestine [23]. Both overexpression and knockout of the *Muc1* gene has been associated with the development of different cancer diseases [41–43], but have also been reported to be associated with anti-inflammatory effects by regulating toll-like receptor (TLR) expressions [44,45]. *A. muciniphila* is a mucin-degrading bacteria and have been suggested to have beneficial impact on human health, of which is linked to the regulation of the mucus thickness and gut barrier integrity [46]. Hence, it could be speculated that additional degradation of mucin by the administered AKM strain regulated the expression of *Muc1* to a neither over-expressive nor over-suppressive level.

The FVT treated mice were unexpectedly associated with a significantly ($p < 0.05$) increased fertility rate (Figure 6A) and pregnancy status (Figure 6B). The study was not designed to investigate fertility rates which also are reflected by the group sizes. Both the male and female mice were treated with FVT; thus, the basic premises of the experimental setup make it challenging to evaluate if the increased fertility rate and pregnancy status were due to improved sperm quality of the males and/or improved conditions for fertility in the female mice. Emerging evidence suggest that infertility should be added to the list of GM associated diseases [47–49], and the importance of validating this link to the GM is emphasized by infertility being estimated to affect up to 15% of couples world-wide [50,51]. Our observations are in line with other studies suggesting a link between fertility and the GM, e.g. the demonstrated improvement of spermatogenesis with FMT from healthy donors [52], as well as, impairment of spermatogenesis with FMT from donors with a dysbiotic GM [47]. In regard to females, links have been suggested between maternal obesity, gut dysbiosis, and inflammation [49]. New results have discovered a markedly increase in the abundance of *Bacteroides vulgatus* in the gut of polycystic ovary syndrome (PCOS) individuals, that through deconjugations of bile acids in the liver affects the interleukin-22 (IL-22) levels and ultimately the fertility [48]. Although additional experiments need to be conducted, it cannot be ruled out, that the transfer of AKM in the

AKM+Saline mice led to similar cascading events that might have decreased the fertility of the male and/or female mice (Figure 6).

Conclusively, we here demonstrate that FVT increases the abundance of, what is expected to be, naturally occurring *A. muciniphila* strains in the recipient mice. The bulk and undefined nature of fecal viromes prevents any direct use as a commercial product. However, our results highlight the potential of using phage-mediated changes of the GM as a supplement to probiotics to enhance the growth of healthy commensals that outside the body are defined as probiotics. Furthermore, an unexpected event of increased fertility rate and pregnancy status was associated to the FVT treatment, which urge for additional studies specifically designed to clarify our observations.

Methods

Bacterial strains

The commercially available probiotic bacterium *Lacticaseibacillus rhamnosus* GG (LMG 18243, former *Lactobacillus rhamnosus* [53]) was included along with *Akkermansia muciniphila* YL-44 (DSM 26127), as a representative of next-generation probiotics [54].

Preparation of inocula of L. rhamnosus (LGG) and A. muciniphila (AKM) for transfer to mice

L. rhamnosus GG (LGG) and *A. muciniphila* YL-44 (AKM) were both handled and incubated anaerobically as described previously [55]. AKM was incubated in Gifu Anaerobic Medium (GAM, HyServe, cat. no. 5422) and LGG in de Man Rogosa Sharpe broth (MRS, Merck, cat. no. 69966) in broth or agar plates containing 1.5% agar. In brief, GAM or MRS broth were boiled prior to distribution in Hungate tubes (SciQuip, cat. no. 2047-16125), and subsequently flushes with 100% N_2 with an anaerobic gassing unit (QCAL Messtechnik GmbH, Munich, Germany) for at least 3 min per 10 mL. Both liquid and solid media contained 0.02% (w/v) 1,4-dithiothreitol (Merck, cat. No. DTT-RO) and 0.05% (w/v) L-cysteine (Merck, cat. no. 168149) as reducing agents and 1 mg/L resazurin as oxygen indicator. All media were autoclaved (121°C for 20 min). Anaerobic handling of cultures was performed in an anaerobic chamber (Model AALC, Coy Laboratory Products, Grass Lake, Michigan, USA) containing ~93% (v/v) N_2, ~2% H_2, ~5% CO_2 at room temperature (RT), and agar plates were incubated in an anaerobic jar (Thermo Scientific, cat. no. HP0011A,) along with an anaerobic sachet (Thermo Scientific, AnaeroGen™ cat. no. AN0035A). Incubation of tubes as well

as plates was performed at 37°C. For preparing the probiotic solutions, a single bacterial colony was inoculated to the growth medium and incubated until the stationary phase was reached after 24 hours for LGG or 72 hours for AKM. This was followed by a 2% (v/v) culture incubation until the exponential phase was reached after 12 hours for LGG or 48 hours for AKM. The bacterial concentrations were measured with an optical density at 600 nm (OD_{600}) with Genesys™ 30 Visible spectrophotometer (Thermo Scientific, cat. no. 840-277000, Waltham, Massachusetts, USA) mounted with a test-tube holder (VWR, cat. no. 634-0911). To ensure high bacterial loads in the probiotic inocula, the bacterial cultures were upconcentrated 40x by centrifugation at 4450 x g for 30 min at RT under anaerobic conditions and resuspended in anaerobic Intralipid®. Intralipid® was used to protect the viable bacterial cells against the acidic environment in the mouse upper gastrointestinal tract [56] and an oil-water emulsion solution was made by mixing the resuspended bacterial cultures with a 3-way stopcock (Braun, Discofix® cat. no. 409511). Pure Intralipid® was used as the probiotic sham (Pro-sham). Small single-use vials of the probiotic solutions were prepared for each mouse to minimize the introduction of oxygen when administering the probiotics. The probiotic solutions were freshly prepared for both the 1st and 2nd inoculation which explain the variances in the bacterial colony forming units (CFU)/mL. Phase contrast microscopy images were taken to check for contamination on the cell morphology level (Figure S11). The total CFU transferred to each mouse at 1st inoculation was LGG: 2.8 x 10^8 CFU and AKM: 3.8 x 10^8 CFU and at 2nd inoculation LGG: 5.5 x 10^9 CFU and AKM: 2.0 x 10^9 CFU.

Preparation of donor virome

Fecal viromes were extracted from intestinal content from mice (low-fat diet fed male C57BL/6NCrl and C57BL/6NRj mice) that previously [22] was found with a relative abundance of *A. muciniphila* above 6% and to exhibit inter-vendor variance in their GM profiles [22,57]. The titer of the applied FVT virome was approximately 5.4 x 10^9 virus-like particles (VLP)/mL (Figure S12 and Table S1) for both 1st and 2nd inoculation and was evaluated by epifluorescence microscopy stained by SYBR™ Gold (Thermo Scientific, cat. no. S11494) as previously described (dx.doi.org/10.17504/protocols.io.bx6cpraw). The total VLPs transferred to each mouse per inoculation was 8.0 x 10^8 VLPs. SM buffer (NaCl 200 mM, $MgSO_4 \cdot 7H_2O$ 16 mM, Tris-HCl 100 mM, pH 7.5) was used as viral sham (Saline).

Animal study design

In total 48 C57BL/6NTac mice at 4 weeks old (Taconic, Lille Skensved, Denmark) were included in the study (representing 24 males and 24 females). They were ear tagged upon arrival and divided into six groups: LGG+FVT, AKM+FVT, Pro-sham+FVT, LGG+Saline, AKM+Saline, and control (Pro-sham+Saline) (Figure 1). The Saline consisted of SM buffer and Pro-sham consisted of Intralipid® (Fresenius Kabi, Intralipid® 200 mg/mL) that were used to suspend the probiotic bacteria. The mice were housed in open transparent cages with a wire lid (1290D Eurostandard Type III, Scanbur A/S, Karlslunde, Denmark) with access to bottled tap water *ad libitum*, and the cages were enriched with bedding, cardboard housing, tunnel, nesting material, felt pad, and biting stem (respectively, Cat. no. 30983, 31000, 31003, 31008, 31007, 30968 Brogaarden). The mice were fed *ad libitum* chow diet (Altromin 1324, Brogaarden) during the entire 6 weeks of the study. Health monitoring of animals was performed without revealing any pathogens according to FELASA guidelines [58]. Cages were changed weekly. The mice were housed in male-female pairs (in total 24 cages) to evaluate the effect of sex of the animals on the interventions, increase animal welfare by eliminating aggression between co-housed males, and by consequence also allowed natural mating behavior. After a week of acclimatization, the mice were inoculated orally using a pipette with 50 µl 1M bicarbonate solution (Merck, cat. no. S5761) that 5 min later was followed by oral gavage with 0.15 mL FVT/Saline solutions (FVT/Saline, n = 24). The following day the mice were inoculated orally by gently using a pipette with 100 µL probiotic solution of AKM/LGG/Pro-sham (AKM/Pro-sham, n=16 and LGG/Pro-sham, n=16), which constituted the 1st inoculation. The same procedures were repeated in the 2nd inoculation a week after. The mice were weighted, and fecal samples were taken at several timepoints during the study, amongst other at baseline, 6 days after 2nd intervention, and at termination. The fecal samples were stored at -80°C. One female mouse (representing the AKM+FVT group) was sacrificed following the first probiotic inoculation due to suffering. At termination (9 weeks of age), the remaining 47 mice were anesthetized with a hypnorm/midazolam mixture. Both hypnorm (Hypnorm BN: P736/005, VetaPharma Ltd, Leeds, UK) and midazolam were mixed with sterile water in a ratio of 1:1 (BN: 353 0418, Braun, Melsungen, Germany). The animals were euthanized by cervical dislocation. The mesenteric lymph node (MLN) was sampled in ice cold PBS and 2 cm of the distal ileum was sampled in two pieces and snap frozen in liquid nitrogen and stored in -80°C. Surgical equipment used for tissue and fecal sampling during terminal procedures was sterilized between each animal. Pups, both born and *in utero* were counted and euthanized by decapitation. The study was approved by the Danish Competent Authority, The Animal

Experimentation Inspectorate, under the Ministry of Environment and Food of Denmark, and performed under license No. 2017-15-0201-01262 C1-3. Procedures were carried out in accordance with the Directive 2010/63/EU and to the Danish law LBK Nr 726 af 09/091993, and housing conditions as earlier described [22].

Gene expression assay

Ileum (1 cm) pieces were transferred to tubes (Mpbio, cat. no. FastPrep® 50-76-200) including 0.6g glass beads (Sigma-Aldrich, cat. no. G4649), 600 µl lysis binding solution concentrate (Invitrogen™, cat. no. AM1830) and 0.7% β-mercaptoethanol (Sigma-Aldrich, cat. no. M6250) and homogenized on the FastPrep-24™ Classic Instrument (Mpbio, Irvine, California, USA) with 4 x (45 sec at speed 6.5 m/s) runs. The homogenate was centrifuged at 16,000 x g and the supernatant was frozen at -20°C for at least 24 hours before purification of RNA using the MagMax™ Express Magnetic Particle Processor (Applied Biosystems™, Waltham, Massachusetts, USA) using manufacturer's instructions (Invitrogen™, cat. no. AM1830). RNA purity and concentration were assessed using DeNovix DS11 Fx+ Spectrophotomer (DeNovix, Wilmington, USA) and intact 18S rRNA and 28S rRNA bands was visually inspected on a 1.4% agarose gel. cDNA was synthesized from 500 ng total RNA with the High-capacity cDNA reverse Transcription Kit (Applied Biosystems™, Waltham, Massachusetts, USA) in a reaction volume of 20 µl following manufacturers recommendations. 2 -RT controls were prepared without the Reverse transcriptase enzyme and cDNA samples was diluted 8x after synthesis. High throughput qPCR was run on duplicates on the Biomark HD system (Fluidigm Corporation, South San Francisco, California, USA) on 2x 96.96 IFC chips on pre-amplified cDNA duplicates using manufacturer's instructions with minor adjustments as previously described [59]. The majority of the primers in the Ileum primer panel was previously published [17]. 81 primer assays (74 candidate genes, 7 reference genes, 1 gDNA control assay) (see Supplementary file 1 for the full list) were present with one product and had a sufficient efficiency between 75-110%. In addition, the MVP1 gene assay was included to control for gDNA contamination [60]. qPCR data was analyzed as previously described and normalized to the four most stable reference genes: Sdha, Tuba, Pgk1, Ppia [17,59]. A log2 fold change threshold was set to 0.5 and the FDR p-value to 0.05 for gene expressions to be included in the analysis.

Cell isolation and flow cytometry (FACS)

Directly after euthanasia of the mice, the mesenteric lymph node (MLN) was placed in ice cold PBS. Single cell suspensions were prepared by disrupting the lymph node between two microscope glasses and passing it through a 70 µm nylon mesh. After washing and resuspension, 1x106 cells were surface stained for 30 min with antibodies for Percp-Cy5.5 conjugated CD11c, PE-conjugated CD86, APC-conjugated CD11b, and FITC-conjugated CD103 (all antibodies were purchased from eBiosciences, San Diego, CA USA) for the detection of tolerogenic dendritic cells (DCs). For the detection of T cell subsets, 1x106 cells were initially surface stained for 30 min with FITC-conjugated CD3, PercP-Cy5.5-conjugated CD4, and APC-conjugated CD8a (ebiosciences), then fixate and permeabilized with the FoxP3/Transcription Facter Staining Buffer Set (ebiosciences), and finally stained for 30 min with PE-conjugated intracellular forkhead box P3 (FOXP3) (ebioscience). Analysis was performed using an Accuri C6 flow cytometer (Accuri Cytometers, Ann Arbor, MI, USA).

Pre-processing of fecal samples

Fecal samples from three different timepoints were included to investigate GM changes over time: baseline, after intervention, and at termination. This represented in total 142 fecal samples from the C57BL/6NTac mice. Separation of the viruses and bacteria from the fecal samples generated a fecal pellet and fecal supernatant as earlier described [22].

Quantitative real-time PCR for measuring probiotic density

The bacterial density of AKM and LGG in the fecal samples was estimated using quantitative real-time polymerase chain reaction (qPCR) with species specific primers (AKM_Fwd: 5'-CCT TGC GGT TGG CTT CAG AT-3' and AKM_Rev: 5'-CAG CAC GTG AAG GTG GGG AC-3' [61] and LGG_Fwd: 5'-GCC GAT CGT TGA CGT TAG TTG G-3' and LGG_Rev: 5'-CAG CGG TTA TGC GAT GCG AAT-3' [62]) purchased from Integrated DNA Technologies (IDT, Iowa, USA). Standard curves (Table S2) were based on a dilution series of total DNA extracted from monocultures of AKM and LGG. The qPCR results were obtained using the CFX96 Touch Real-Time PCR Detections System (Bio-Rad Laboratories, Hercules, California, USA) and the reagent SsoFast™ EvaGreen® Supermix with Low ROX (Bio-Rad Laboratories, cat. no. 1725211), and run as previously described [63].

Bacterial DNA extraction, sequencing and pre-processing of raw data

The Bead-Beat Micro AX Gravity kit (A&A Biotechnology, cat. no. 106-100 mod.1) was used to extract bacterial DNA from the fecal pellet by following the instructions of the manufacturer. The final purified DNA was stored at -80ºC and the DNA concentration was determined using Qubit HS Assay Kit on the Qubit 4 Fluorometric Quantification device (Invitrogen, Carlsbad, California, USA). The bacterial community composition was determined by Illumina NextSeq-based high-throughput sequencing (HTS) of the 16S rRNA gene V3-region, as previously described [22]. Quality-control of reads, de-replicating, purging from chimeric reads and constructing zOTU was conducted with the UNOISE pipeline [64] and taxonomically assigned with Sintax [65] (not yet peer reviewed). Taxonomical assignments were obtained using the EZtaxon for 16S rRNA gene database [66]. Code describing this pipeline can be accessed in github.com/jcame/Fastq_2_zOTUtable. The average sequencing depth after quality control (Accession: PRJEB52388, available at ENA) for the fecal 16S rRNA gene amplicons was 47,526 reads (min. 6,588 reads and max. 123,389 reads).

Viral DNA extraction, sequencing and pre-processing of raw data

The sterile filtered fecal supernatant was concentrated using Centriprep® filter units (Merck, cat. no. 4311 and cat. no. 4307). This constituted the concentrated virome. Due to a permanent stop in the production of Centriprep® filter units at the manufacturer, we were forced to use residual stocks of filter size 30 kDa (cat. no. 4307) for 42% of the samples (Table S3). The samples were all centrifuged at 1500 x g at 15ºC until approx. 500 µL concentrated virome sample was left, the filter was removed with a sterile scalpel and stored along with the concentrated virome at 4ºC. Viral DNA was extracted, multiple displacement amplification (MDA, to include ssDNA viruses), and Illumina NextSeq sequencing data generated as previously described [22]. The average sequencing depth after quality control (Accession: PRJEB52388, available at ENA) for the fecal viral metagenome was 209,641 reads (min. 21,580 reads and max. 510,332 reads. The raw reads were trimmed from adaptors and the high quality sequences (>95% quality) using Trimmomatic v0.35 [67] with a minimum size of 50nt were retained for further analysis. High quality reads were de-replicated and checked for the presence of PhiX control using BBMap (bbduk.sh) (https://www.osti.gov/servlets/purl/1241166). Virus-like particle-derived DNA sequences were subjected to within-sample de-novo assembly-only using Spades v3.13.1 [68] and the contigs with a minimum length of 2,200 nt, were retained. Contigs generated from all samples were pooled and de-replicated at 90% identity using BBMap (dedupe.sh). Prediction of viral contigs/genomes was carried out using VirSorter2 [69] ("full" categories |

433 dsDNAphage, ssDNA, RNA, Lavidaviridae, NCLDV | viralquality ≥ 0.66), vibrant [70] (High-
434 quality | Complete), and checkv [71] (High-quality | Complete). Taxonomy was inferred by blasting
435 viral ORF against viral orthologous groups (https://vogdb.org) and the Lowest Common Ancestor
436 (LCA) for every contig was estimated based on a minimum e-value of $10e^{-5}$. Phage-host prediction
437 was determined by blasting (85% identity) CRISPR spacers and tRNAs predicted from >150,000 gut
438 species-level genome bins (SGBs) [72,73] ([73], not yet peer reviewed). Following assembly, quality
439 control, and annotations, reads from all samples were mapped against the viral (high-quality) contigs
440 (vOTUs) using the bowtie2 [74] and a contingency-table of reads per Kbp of contig sequence per
441 million reads sample (RPKM) was generated, here defined as vOTU-table (viral contigs). Code
442 describing this pipeline can be accessed in github.com/jcame/virome_analysis-FOOD.

443 ***Bioinformatic analysis of bacterial and viral DNA sequences***

444 Initially the RPKM normalized dataset was purged for viral contigs which were detected in less than
445 5% of the samples, but the resulting dataset still maintained 99.5% of the total reads. Cumulative sum
446 scaling (CSS) [75] was applied for the analysis of β-diversity to counteract that a few viral contigs
447 represented a majority of count values, since CSS have been benchmarked with a high accuracy for
448 the applied metrics [76]. CSS normalization was performed using the R software using the
449 metagenomeSeq package [77]. A-diversity analysis was based on raw read counts and statistics were
450 based on ANOVA. R version 4.01 [78] was used for subsequent analysis and presentation of data.
451 The data are uploaded as supplementary data (www.osf.oi/tm2a5). The main packages used were
452 phyloseq [79], vegan [80], deseq2 [81], ampvis2 [82] (not yet peer reviewed), ggpubr [83], mctoolsr
453 (`https://github.com/leffj/mctoolsr/`), and ggplot2 [84]. B-diversity was represented by Bray
454 Curtis dissimilarity and statistics were based on PERMANOVA. A linear model
455 (y~FVT+probiotics+sex), similar to ANOVA, was applied to assess the statistically differences
456 between the treatment groups of gene expression, bacterial abundance, immune cell counts, and
457 fertility rate. Two treatment groups were applied in the model; a FVT group (levels: control and FVT)
458 and a probiotic group (levels: control, AKM and LGG). The sex of the animal was added as an
459 additional factor, except for fertility outcome analysis where only females were included. For binary
460 outcomes a generalized logistic regression model was applied.

Acknowledgements

We thank the animal caretakers Helene Farlov and Mette Nelander at Section of Experimental Animal Models (University of Copenhagen, Denmark) for taking care of the animals during the study and assisting with the animal handling.

Funding

Funding was provided by the Danish Council for Independent Research with grant ID: DFF-6111-00316 “PhageGut” (www.phagegut.ku.dk).

Author contributions

TSR, CMJM, AKH, and DSN conceived the research idea and designed the study; TSR, CMJM, MRD, LSFZ, performed the experiments TSR, CMJM, MRD, RRJ, LSFZ, JLCM, LHH, AKH, and DSN performed laboratory and data analysis; TSR wrote the first draft of the manuscript. All authors critically revised and approved the final version of the manuscript.

Competing interests

All authors declare no conflicts of interest.

Data availability statement

Supplementary materials and raw data used for the analysis can be accessed through doi: 10.17605/OSF.IO/TM2A5 (www.osf.oi/tm2a5). Raw sequencing data can be accesses at ENA with project ID: PRJEB52388 (https://www.ebi.ac.uk/ena/browser/).

References

1 Ley RE, Turnbaugh PJ, Klein S, *et al.* Microbial ecology: human gut microbes associated with obesity. *Nature* 2006;**444**:1022–3. doi:10.1038/4441022a

2 Kang D-W, Adams JB, Coleman DM, *et al.* Long-term benefit of microbiota transfer therapy on autism symptoms and gut microbiota. *Sci Rep* 2019;**9**:5821. doi:10.1038/s41598-019-42183-0

3 Nakatsu G, Zhou H, Wu WKK, *et al.* Alterations in enteric virome are associated with colorectal cancer and survival outcomes. *Gastroenterology* 2018;**155**:529-541.e5. doi:10.1053/j.gastro.2018.04.018

4 Reid JNS, Bisanz JE, Monachese M, *et al.* The rationale for probiotics improving reproductive health and pregnancy outcome. *Am J Reprod Immunol* 2013;**69**:n/a-n/a. doi:10.1111/aji.12086

5 Valcarce DG, Genovés S, Riesco MF, *et al.* Probiotic administration improves sperm quality in asthenozoospermic human donors. *Benef Microbes* 2017;**8**:193–206. doi:10.3920/BM2016.0122

6 Martín R, Langella P. Emerging health concepts in the probiotics field: Streamlining the definitions. *Front Microbiol* 2019;**10**. doi:10.3389/fmicb.2019.01047

7 Katan MB. Why the European Food Safety Authority was right to reject health claims for probiotics. *Benef Microbes* 2012;**3**:85–9. doi:10.3920/BM2012.0008

8 Zhao S, Liu W, Wang J, *et al. Akkermansia muciniphila* improves metabolic profiles by reducing inflammation in chow diet-fed mice. *J Mol Endocrinol* 2017;**58**:1–14. doi:10.1530/JME-16-0054

9 Everard A, Belzer C, Geurts L, *et al.* Cross-talk between *Akkermansia muciniphila* and intestinal epithelium controls diet-induced obesity. *Proc Natl Acad Sci U S A* 2013;**110**:9066–71. doi:10.1073/pnas.1219451110

10 Scott CJ, Kardon RH, Lee AG, *et al.* Diagnosis and grading of papilledema in patients with raised intracranial pressure using optical coherence tomography vs clinical expert assessment using a clinical staging scale. *Arch Ophthalmol (Chicago, Ill 1960)* 2010;**128**:705–11. doi:10.1001/archophthalmol.2010.94

11 Kristensen NB, Bryrup T, Allin KH, *et al.* Alterations in fecal microbiota composition by probiotic supplementation in healthy adults: a systematic review of randomized controlled trials. *Genome Med* 2016;**8**:52. doi:10.1186/s13073-016-0300-5

12 Howe A, Ringus DL, Williams RJ, *et al.* Divergent responses of viral and bacterial communities in the gut microbiome to dietary disturbances in mice. *ISME J* 2016;**10**:1217–27. doi:10.1038/ismej.2015.183

13 Scarpellini E, Ianiro G, Attili F, *et al.* The human gut microbiota and virome: Potential therapeutic implications. *Dig Liver Dis* 2015;**47**:1007–12. doi:10.1016/j.dld.2015.07.008

14 Reyes A, Haynes M, Hanson N, *et al.* Viruses in the faecal microbiota of monozygotic twins and their mothers. *Nature* 2010;**466**:334–8. doi:10.1038/nature09199

15 Barrangou R, Yoon S-S, Breidt F, *et al.* Characterization of six *Leuconostoc fallax* bacteriophages isolated from an industrial sauerkraut fermentation. *Appl Environ Microbiol* 2002;**68**:5452–8. doi:10.1128/AEM.68.11.5452-5458.2002

16 Ott SJ, Waetzig GH, Rehman A, *et al.* Efficacy of sterile fecal filtrate transfer for treating patients with *Clostridium difficile* infection. *Gastroenterology* 2017;**152**:799-811.e7. doi:10.1053/j.gastro.2016.11.010

17 Rasmussen TS, Mentzel CMJ, Kot W, *et al.* Faecal virome transplantation decreases symptoms of type 2 diabetes and obesity in a murine model. *Gut* 2020;**69**:2122–30. doi:10.1136/gutjnl-2019-320005

18 Brunse A, Deng L, Pan X, *et al.* Fecal filtrate transplantation protects against necrotizing enterocolitis. *ISME J* 2022;**16**:686–94. doi:10.1038/s41396-021-01107-5

19 Zuo T, Wong SH, Lam K, *et al.* Bacteriophage transfer during faecal microbiota transplantation in *Clostridium difficile* infection is associated with treatment outcome. *Gut* 2018;**67**:634–43. doi:10.1136/gutjnl-2017-313952

20 Rasmussen TS, Koefoed AK, Jakobsen RR, *et al.* Bacteriophage-mediated manipulation of the gut microbiome - promises and presents limitations. *FEMS Microbiol Rev* 2020;**44**:507–21. doi:10.1093/femsre/fuaa020

21 Draper LA, Ryan FJ, Dalmasso M, *et al.* Autochthonous faecal viral transfer (FVT) impacts the murine microbiome after antibiotic perturbation. *BMC Biol* 2020;**18**:173. doi:10.1186/s12915-020-00906-0

22 Rasmussen TS, de Vries L, Kot W, *et al.* Mouse vendor influence on the bacterial and viral gut composition exceeds the effect of diet. *Viruses* 2019;**11**:435. doi:10.3390/v11050435

23 Dhar P, McAuley J. The role of the cell surface mucin MUC1 as a barrier to infection and regulator of inflammation. *Front Cell Infect Microbiol* 2019;**9**:117. doi:10.3389/fcimb.2019.00117

24 Lynn MA, Eden G, Ryan FJ, *et al.* The composition of the gut microbiota following early-life antibiotic exposure affects host health and longevity in later life. *Cell Rep* 2021;**36**:109564. doi:10.1016/j.celrep.2021.109564

25 Wang J, Lang T, Shen J, *et al.* Core gut bacteria analysis of healthy mice. *Front Microbiol* 2019;**10**:887. doi:10.3389/fmicb.2019.00887

26 Daly C, Rollins BJ. Monocyte chemoattractant protein-1 (CCL2) in inflammatory disease and adaptive immunity: therapeutic opportunities and controversies. *Microcirculation* 2003;**10**:247–57. doi:10.1038/sj.mn.7800190

27 Wu Q, Chen J-X, Chen Y, *et al.* The chemokine receptor CCR10 promotes inflammation-driven hepatocarcinogenesis via PI3K/Akt pathway activation. *Cell Death Dis* 2018;**9**:232. doi:10.1038/s41419-018-0267-9

28 Verhagen J, Sabatos CA, Wraith DC. The role of CTLA-4 in immune regulation. *Immunol Lett* 2008;**115**:73–4. doi:10.1016/j.imlet.2007.10.010

29 Łukaszewicz-Zając M, Pączek S, Mroczko P, *et al.* The significance of CXCL1 and CXCL8 as well as their specific receptors in colorectal cancer. *Cancer Manag Res* 2020;**Volume 12**:8435–43. doi:10.2147/CMAR.S267176

30 Ren K, Torres R. Role of interleukin-1beta during pain and inflammation. *Brain Res Rev* 2009;**60**:57–64. doi:10.1016/j.brainresrev.2008.12.020

31 Brown MA, Hural J. Functions of IL-4 and control of its expression. *Crit Rev Immunol* 1997;**17**:1–32. doi:10.1615/critrevimmunol.v17.i1.10

32 Tanaka T, Narazaki M, Kishimoto T. IL-6 in inflammation, immunity, and disease. *Cold Spring Harb Perspect Biol* 2014;**6**:a016295. doi:10.1101/cshperspect.a016295

33 Pine GM, Batugedara HM, Nair MG. Here, there and everywhere: Resistin-like molecules in infection, inflammation, and metabolic disorders. *Cytokine* 2018;**110**:442–51. doi:10.1016/j.cyto.2018.05.014

34 Knight BE, Kozlowski N, Havelin J, *et al.* TIMP-1 attenuates the development of inflammatory pain through MMP-dependent and receptor-mediated cell signaling mechanisms. *Front Mol Neurosci* 2019;**12**:1–16. doi:10.3389/fnmol.2019.00220

35 Bartoszek A, Moo E Von, Binienda A, *et al.* Free Fatty Acid Receptors as new potential

therapeutic target in inflammatory bowel diseases. *Pharmacol Res* 2020;**152**:104604. doi:10.1016/j.phrs.2019.104604

36 Sivaprakasam S, Gurav A, Paschall A V, *et al.* An essential role of Ffar2 (Gpr43) in dietary fibre-mediated promotion of healthy composition of gut microbiota and suppression of intestinal carcinogenesis. *Oncogenesis* 2016;**5**:e238. doi:10.1038/oncsis.2016.38

37 Rodriguez-Nunez I, Caluag T, Kirby K, *et al.* Nod2 and Nod2-regulated microbiota protect BALB/c mice from diet-induced obesity and metabolic dysfunction. *Sci Rep* 2017;**7**:548. doi:10.1038/s41598-017-00484-2

38 Grubb DS, Wrigley SD, Freedman KE, *et al.* PHAGE-2 Study: Supplemental bacteriophages extend *Bifidobacterium animalis* subsp. lactis BL04 benefits on gut health and microbiota in healthy adults. *Nutrients* 2020;**12**. doi:10.3390/nu12082474

39 Chen L, Deng H, Cui H, *et al.* Inflammatory responses and inflammation-associated diseases in organs. *Oncotarget* 2018;**9**:7204–18. doi:10.18632/oncotarget.23208

40 Moro-García MA, Mayo JC, Sainz RM, *et al.* Influence of inflammation in the process of T lymphocyte differentiation: proliferative, metabolic, and oxidative changes. *Front Immunol* 2018;**9**:339. doi:10.3389/fimmu.2018.00339

41 Nath S, Mukherjee P. MUC1: a multifaceted oncoprotein with a key role in cancer progression. *Trends Mol Med* 2014;**20**:332–42. doi:10.1016/j.molmed.2014.02.007

42 Xu X, Chen W, Leng S, *et al.* Muc1 knockout potentiates murine lung carcinogenesis involving an epiregulin-mediated EGFR activation feedback loop. *Carcinogenesis* 2017;**38**:604–14. doi:10.1093/carcin/bgx039

43 Sahraei M, Bose M, Sanders JA, *et al.* Repression of MUC1 promotes expansion and suppressive function of myeloid-derived suppressor cells in pancreatic and breast cancer murine models. *Int J Mol Sci* 2021;**22**:1–15. doi:10.3390/ijms22115587

44 Kyo Y, Kato K, Park YS, *et al.* Antiinflammatory role of MUC1 mucin during infection with nontypeable *Haemophilus influenzae*. *Am J Respir Cell Mol Biol* 2012;**46**:149–56. doi:10.1165/rcmb.2011-0142OC

45 Lindén SK, Florin THJ, McGuckin MA. Mucin dynamics in intestinal bacterial infection. *PLoS One* 2008;**3**:e3952. doi:10.1371/journal.pone.0003952

46 Trastoy B, Naegeli A, Anso I, *et al.* Structural basis of mammalian mucin processing by the human gut O-glycopeptidase OgpA from *Akkermansia muciniphila*. *Nat Commun* 2020;**11**:4844. doi:10.1038/s41467-020-18696-y

47 Ding N, Zhang X, Zhang X Di, *et al.* Impairment of spermatogenesis and sperm motility by the high-fat diet-induced dysbiosis of gut microbes. *Gut* 2020;**69**:1608–19. doi:10.1136/gutjnl-2019-319127

48 Qi X, Yun C, Sun L, *et al.* Gut microbiota-bile acid-interleukin-22 axis orchestrates polycystic ovary syndrome. *Nat Med* 2019;**25**:1225–33. doi:10.1038/s41591-019-0509-0

49 Davis JS. Connecting female infertility to obesity, inflammation, and maternal gut dysbiosis. *Endocrinology* 2016;**157**:1725–7. doi:10.1210/en.2016-1198

50 Agarwal A, Mulgund A, Hamada A, *et al.* A unique view on male infertility around the globe. *Reprod Biol Endocrinol* 2015;**13**:37. doi:10.1186/s12958-015-0032-1

51 Elhussein OG, Ahmed MA, Suliman SO, *et al.* Epidemiology of infertility and characteristics of infertile couples requesting assisted reproduction in a low-resource setting in Africa, Sudan. *Fertil Res Pract* 2019;**5**:7. doi:10.1186/s40738-019-0060-1

52 Zhang P, Feng Y, Li L, *et al.* Improvement in sperm quality and spermatogenesis following faecal microbiota transplantation from alginate oligosaccharide dosed mice. *Gut* 2021;**70**:222–5. doi:10.1136/gutjnl-2020-320992

53 Zheng J, Wittouck S, Salvetti E, *et al.* A taxonomic note on the genus *Lactobacillus*: Description of 23 novel genera, emended description of the genus *Lactobacillus Beijerinck* 1901, and union of *Lactobacillaceae* and *Leuconostocaceae*. *Int J Syst Evol Microbiol* 2020;**70**:2782–858. doi:10.1099/ijsem.0.004107

54 Cani PD, de Vos WM. Next-generation beneficial microbes: the case of *Akkermansia muciniphila*. *Front Microbiol* 2017;**8**:1765. doi:10.3389/fmicb.2017.01765

55 Rasmussen TS, Streidl T, Hitch TCAA, *et al. Sporofaciens musculi* gen. nov., sp. nov., a novel bacterium isolated from the caecum of an obese mouse. *Int J Syst Evol Microbiol* 2021;**71**:004673. doi:10.1099/ijsem.0.004673

56 Nguyen TLA, Vieira-Silva S, Liston A, *et al.* How informative is the mouse for human gut microbiota research? *Dis Model Mech* 2015;**8**:1–16. doi:10.1242/dmm.017400

631 57 Rasmussen TS, Jakobsen RR, Castro-Mejía JL, *et al.* Inter-vendor variance of enteric
632 eukaryotic DNA viruses in specific pathogen free C57BL/6N mice. *Res Vet Sci* 2021;**136**:1–
633 5. doi:10.1016/j.rvsc.2021.01.022

634 58 Mähler (Convenor) M, Berard M, Feinstein R, *et al.* FELASA recommendations for the
635 health monitoring of mouse, rat, hamster, guinea pig and rabbit colonies in breeding and
636 experimental units. *Lab Anim* 2014;**48**:178–92. doi:10.1177/0023677213516312

637 59 Mentzel CMJ, Cardoso TF, Pipper CB, *et al.* Deregulation of obesity-relevant genes is
638 associated with progression in BMI and the amount of adipose tissue in pigs. *Mol Genet*
639 *Genomics* 2018;**293**:129–36. doi:10.1007/s00438-017-1369-2

640 60 Laurell H, Iacovoni JS, Abot A, *et al.* Correction of RT-qPCR data for genomic DNA-
641 derived signals with ValidPrime. *Nucleic Acids Res* 2012;**40**:e51. doi:10.1093/nar/gkr1259

642 61 Greer RL, Dong X, Moraes ACF, *et al. Akkermansia muciniphila* mediates negative effects
643 of IFNγ on glucose metabolism. *Nat Commun* 2016;**7**:13329. doi:10.1038/ncomms13329

644 62 Kim E, Yang S-M, Lim B, *et al.* Design of PCR assays to specifically detect and identify 37
645 *Lactobacillus* species in a single 96 well plate. *BMC Microbiol* 2020;**20**:96.
646 doi:10.1186/s12866-020-01781-z

647 63 Ellekilde M, Krych L, Hansen CHF, *et al.* Characterization of the gut microbiota in leptin
648 deficient obese mice - Correlation to inflammatory and diabetic parameters. *Res Vet Sci*
649 2014;**96**:241–50. doi:10.1016/j.rvsc.2014.01.007

650 64 Edgar RC. Updating the 97% identity threshold for 16S ribosomal RNA OTUs.
651 *Bioinformatics* 2018;**34**:2371–5. doi:10.1093/bioinformatics/bty113

652 65 Edgar R. SINTAX: a simple non-Bayesian taxonomy classifier for 16S and ITS sequences.
653 *bioRxiv* 2016;:074161. doi:10.1101/074161

654 66 Kim O-S, Cho Y-J, Lee K, *et al.* Introducing EzTaxon-e: a prokaryotic 16S rRNA gene
655 sequence database with phylotypes that represent uncultured species. *Int J Syst Evol*
656 *Microbiol* 2012;**62**:716–21. doi:10.1099/ijs.0.038075-0

657 67 Bolger AM, Lohse M, Usadel B. Trimmomatic: A flexible trimmer for Illumina sequence
658 data. *Bioinformatics* 2014;**30**:2114–20. doi:10.1093/bioinformatics/btu170

659 68 Bankevich A, Nurk S, Antipov D, *et al.* SPAdes: a new genome assembly algorithm and its

applications to single-cell sequencing. *J Comput Biol* 2012;**19**:455–77. doi:10.1089/cmb.2012.0021

69 Guo J, Bolduc B, Zayed AA, *et al.* VirSorter2: a multi-classifier, expert-guided approach to detect diverse DNA and RNA viruses. *Microbiome* 2021;**9**:37. doi:10.1186/s40168-020-00990-y

70 Kieft K, Zhou Z, Anantharaman K. VIBRANT: automated recovery, annotation and curation of microbial viruses, and evaluation of viral community function from genomic sequences. *Microbiome* 2020;**8**:90. doi:10.1186/s40168-020-00867-0

71 Nayfach S, Camargo AP, Schulz F, *et al.* CheckV assesses the quality and completeness of metagenome-assembled viral genomes. *Nat Biotechnol* 2021;**39**:578–85. doi:10.1038/s41587-020-00774-7

72 Pasolli E, Asnicar F, Manara S, *et al.* Extensive unexplored human microbiome diversity revealed by over 150,000 genomes from metagenomes spanning age, geography, and lifestyle. *Cell* 2019;**176**:649-662.e20. doi:10.1016/j.cell.2019.01.001

73 Castro-Mejía JL, Khakimov B, Lind M V, *et al.* Gut microbiome and its cofactors are linked to lipoprotein distribution profiles. *bioRxiv* 2021;:2021.09.01.458531. doi:10.1101/2021.09.01.458531

74 Langmead B, Salzberg SL. Fast gapped-read alignment with Bowtie 2. *Nat Methods* 2012;**9**:357–9. doi:10.1038/nmeth.1923

75 Paulson JN, Stine OC, Bravo HC, *et al.* Differential abundance analysis for microbial marker-gene surveys. *Nat Methods* 2013;**10**:1200–2. doi:10.1038/nmeth.2658

76 Weiss S, Xu ZZ, Peddada S, *et al.* Normalization and microbial differential abundance strategies depend upon data characteristics. *Microbiome* 2017;**5**:27. doi:10.1186/s40168-017-0237-y

77 Paulson J. metagenomeSeq: Statistical analysis for sparse high-throughput sequencing. *BioconductorJp* 2014;:1–20.

78 Team RC. R: A language and environment for statistical title.

79 McMurdie PJ, Holmes S. phyloseq: an R package for reproducible interactive analysis and graphics of microbiome census data. *PLoS One* 2013;**8**:e61217.

doi:10.1371/journal.pone.0061217

80 Dixon P. VEGAN, a package of R functions for community ecology. *J Veg Sci* 2003;**14**:927–30. doi:10.1111/j.1654-1103.2003.tb02228.x

81 Love MI, Huber W, Anders S. Moderated estimation of fold change and dispersion for RNA-seq data with DESeq2. *Genome Biol* 2014;**15**:550. doi:10.1186/s13059-014-0550-8

82 Andersen KS, Kirkegaard RH, Karst SM, *et al.* ampvis2: an R package to analyse and visualise 16S rRNA amplicon data. *bioRxiv* April 2018. doi:10.1101/299537

83 Kassambara A. ggpubr: 'ggplot2' based publication ready plots. 2020.https://rpkgs.datanovia.com/ggpubr/ (accessed 30 Jun 2022).

84 Wickham H. ggplot2. *Wiley Interdiscip Rev Comput Stat* 2011;**3**:180–5. doi:10.1002/wics.147

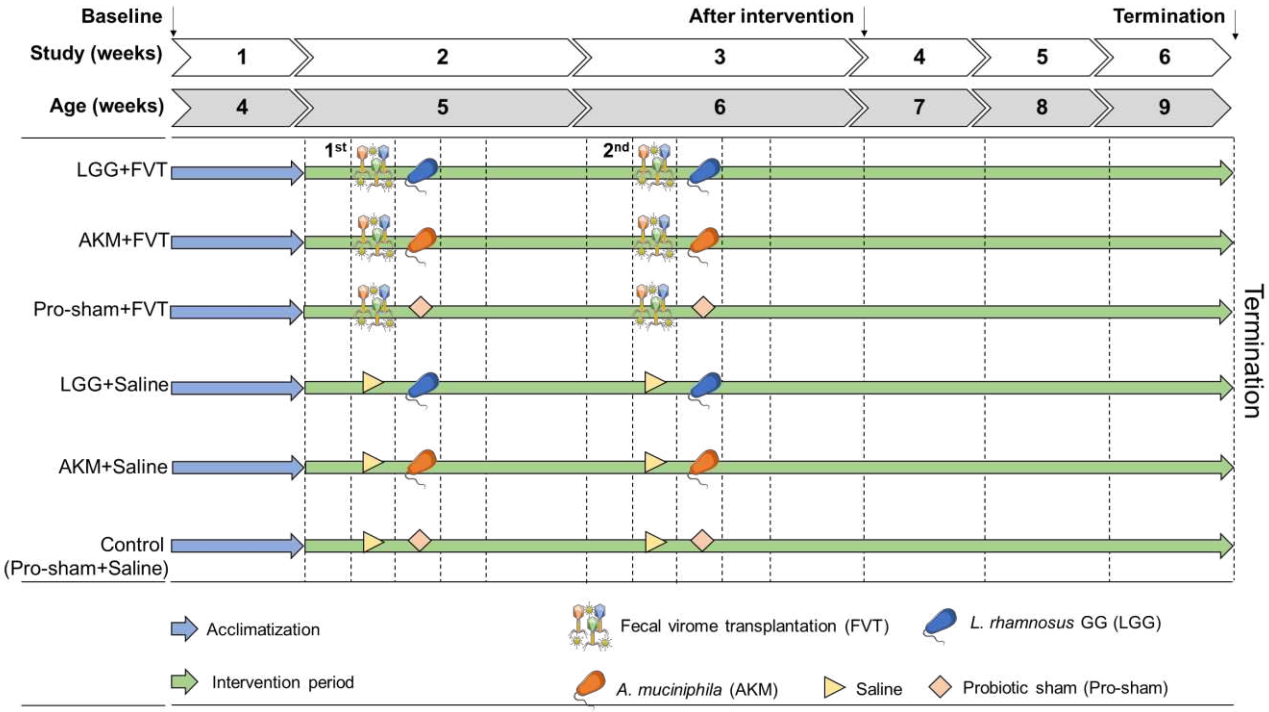

Figure 1: Experimental setup of the animal model. 24 male and 24 female C57BL/6NTac mice (4 weeks old) were divided into six groups: LGG+FVT, AKM+FVT, Pro-sham+FVT, LGG+Saline, and AKM+Saline, control (Pro-sham+Saline). The Saline consisted of SM buffer and Pro-Sham of Intralipid®. The mice were administered 1 M sodium bicarbonate prior oral gavage of FVT/Saline to protect the viral community against the acidic environment in the stomach. The day after, the mice were inoculated with probiotic solutions of LGG/AKM/Pro-sham suspended in Intralipid® which constituted the 1st inoculation. The same procedure was repeated as the 2nd inoculation one week after. The mice were fed *ad libitum* low-fat diet (LFD) for the entire study (6 weeks) until termination at age 9 weeks. Fecal samples from baseline, after intervention, and termination were analyzed in this study. Abbreviations: *Lacticaseibacillus rhamnosus* GG = LGG, *Akkermansia muciniphila* = AKM, fecal virome transplantation = FVT, Pro-sham = probiotic sham.

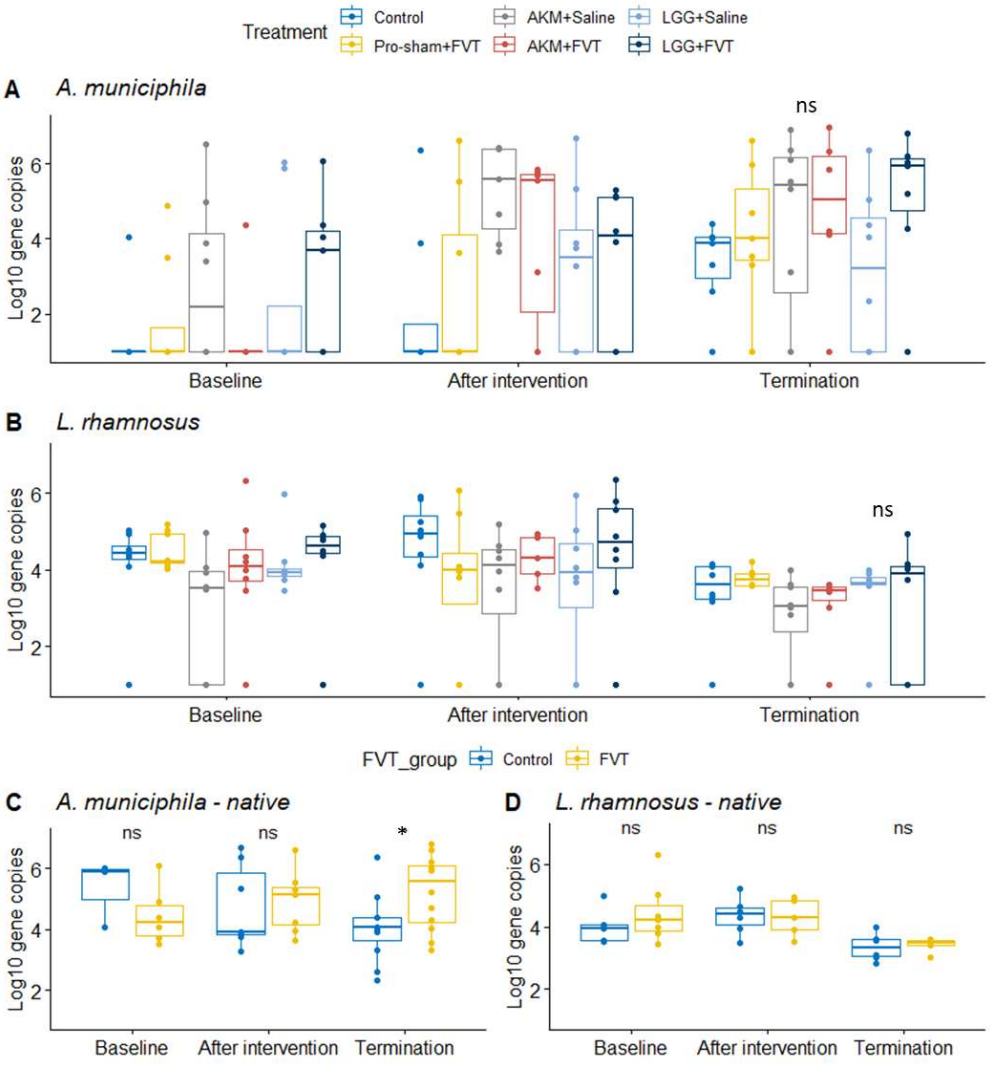

Figure 2: qPCR with *L. rhamnosus* and *A. muciniphila* specific primers were used to assess the abundance of gene copies per gram feces over the time span of baseline, after intervention, and termination. A) The development of the *A. muciniphila* abundance, B) *L. rhamnosus* abundance. C) The abundance development of native *A. muciniphila* strains for mice receiving FVT and no AKM (Pro-sham+FVT and LGG+FVT) compared to not receiving FVT or AKM (LGG+Saline and control). D) The abundance development of native *L. rhamnosus* strains for mice receiving FVT and no LGG (Pro-sham+FVT and AKM+FVT) compared to not receiving FVT or LGG (AKM+Saline and control). Abbreviations: *Lacticaseibacillus rhamnosus* GG = LGG, *Akkermansia muciniphila* = AKM, fecal virome transplantation = FVT, Pro-sham = probiotic sham.

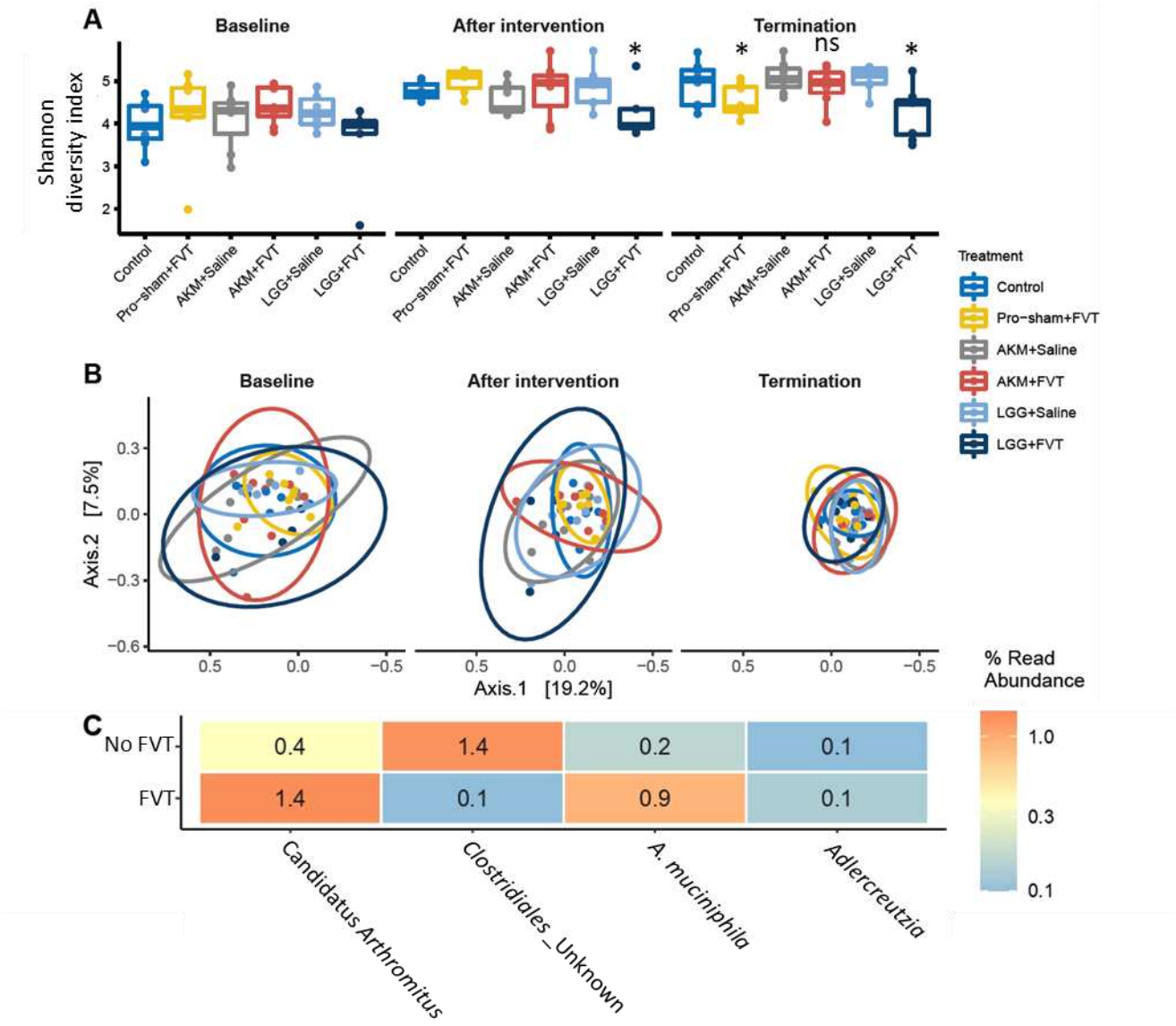

Figure 3: Gut bacteriome analysis of A) the bacterial diversity (Shannon diversity index) and B) PCoA plots of the bacterial composition (Bray Curtis dissimilarity) at baseline, after intervention, and termination. C) Differential abundance analysis of ASVs with significant ($p < 0.05$) different relative abundance between FVT treated mice and mice not receiving FVT. Abbreviations: *Lacticaseibacillus rhamnosus* GG = LGG, *Akkermansia muciniphila* = AKM, fecal virome transplantation = FVT, Pro-sham = probiotic sham, ASV = amplicon sequence variant.

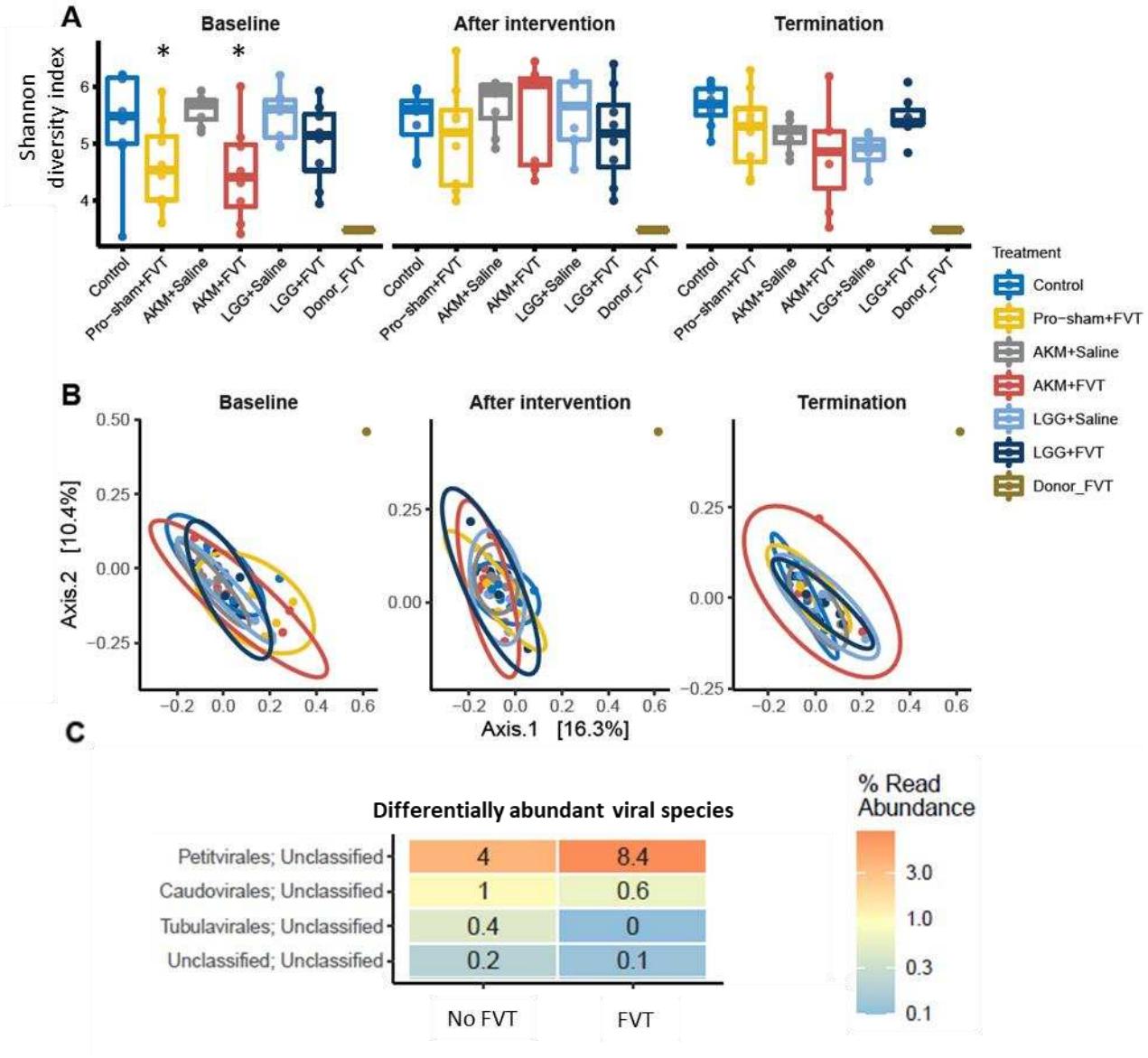

Figure 4: Gut virome analysis of A) the viral diversity (Shannon diversity index) and B) PCoA plots of the viral composition (Bray Curtis dissimilarity) at baseline, after intervention, and termination. C) Differential abundance analysis of viral contigs with significant ($p < 0.05$) different relative abundance between FVT treated mice and mice not receiving FVT. Abbreviations: *Lacticaseibacillus rhamnosus* GG = LGG, *Akkermansia muciniphila* = AKM, fecal virome transplantation = FVT, Pro-sham = probiotic sham.

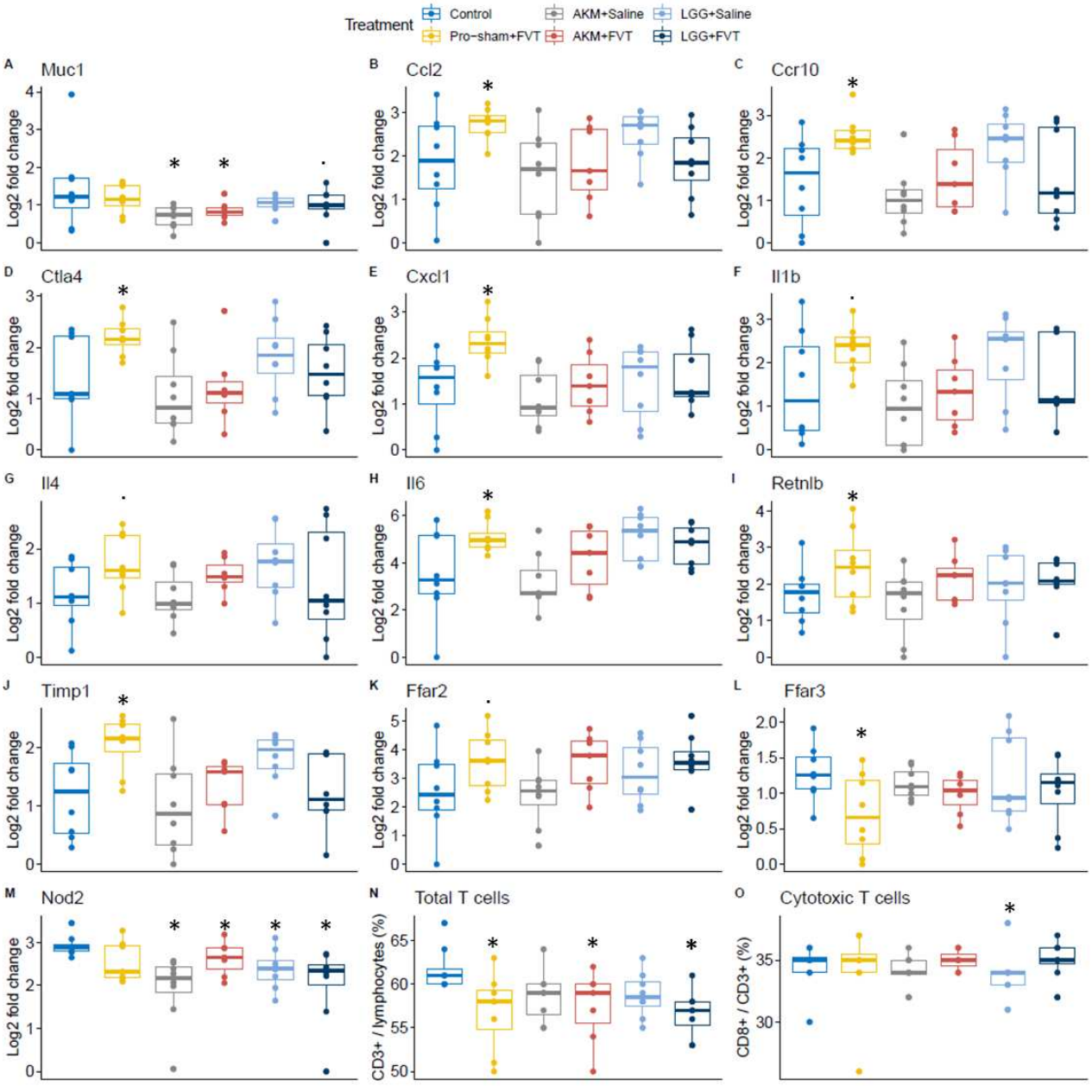

Figure 5: The ileum tissue was investigated for changes in the expressions levels of genes associated to inflammatory responses at termination. In A) to M) the expression levels of these selected genes are shown, and the different treatment groups are compared with the control mice. The relative abundance of total number of T cells N) and cytotoxic T cells (CD8+ T cells) P) were measured. Abbreviations: "*" = ($p < 0.05$), "." = ($p < 0.1$), *Lacticaseibacillus rhamnosus* GG = LGG, *Akkermansia muciniphila* = AKM, fecal virome transplantation = FVT, Pro-sham = probiotic sham.

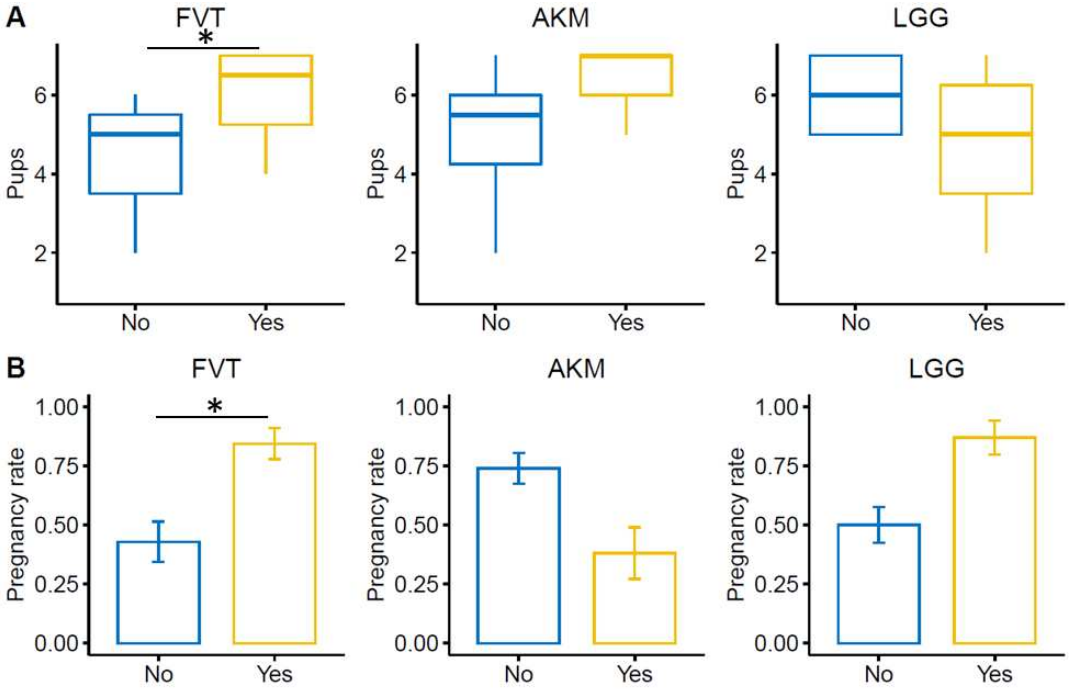

Figure 6: Bar plots of the fertility rate (number of pups) and pregnancy rate. A) The observed number of pups (born or as fetuses) based on a linear model (y~FVT+probiotics). B) The mean distribution of the of the binary event of pregnancy. Only the 23 female mice that received either FVT/Saline along with probiotic solutions of AKM/LGG/Pro-sham was included in the statistical analysis that was based on a generalized logistic regression model (Figure S10). Abbreviations: *Lacticaseibacillus rhamnosus* GG = LGG, *Akkermansia muciniphila* = AKM, fecal virome transplantation = FVT, Pro-sham = probiotic sham, "*" = ($p < 0.05$).